Macro to Nano Tele-Manipulation Through Nanoelectromechanical Systems

Metin Sitti and Hideki Hashimoto

Institute of Industrial Science, University of Tokyo
7-22-1, Roppongi, Minato-ku, Tokyo 106, Japan

Abstract — In this paper, manipulation systems from macroscale world to nanoscale world which are indispensable for constructing Nanoelectromechanical Systems are introduced, and a macro to nano telemanipulation system has been proposed. We selected the tele-robotics manipulation approach for positioning nano objects with sizes between 1 *nm* and 10 *μm* in 2-D. A user interface enables operator to feel the nano forces using a haptic device and see the 3-D graphics of the nano world during the manipulation. Force models, the manipulation strategy and the teleoperation control approach are designed, and preliminary results are presented. Possible target applications of this tele-nanomanipulation system are nanometric particle assembly through constructing 2-D or 3-D NEMS devices, biological object (cell, virus, gene, DNA, etc.) manipulation, and modifying the local surface properties of materials.

1 Introduction

Recent advances on micro-mechatronics technology have enabled microelectromechanical systems (MEMS) where there has been many products recently such as micro pressure sensors and accelerometers for automative industries, microgyroscopes for electronic devices, micro/nano positioning devices such as piezoelectric actuators for precision machining, etc. Utilizing these advances, imaging systems have reached their almost final goal such that Scanning Probe Microscopes (SPM) such as Atomic Force Microscope (AFM) and Scanning Tunneling Microscope (STM) have enabled 3-D visualization down to atomic scale. However, fabrication and manipulation technologies are still immature in manipulating and fabricating micro/nano objects especially within the range of 0.4 *nm* - 10 *μm*. Construction of these technologies in the nanometric scale can enable nanoelectromechanical systems (NEMS) which are the new frontier in miniaturization and can have revolutionary implications in science and technology. NEMS will be extremely small and fast, and have applications in biological systems such as manipulating cells or genes for repairing or understanding mechanisms more clearly, computer industry such as high-density disk storage and miniaturization of integrated circuit components, material science such as fabricating man-made ultrastrong and defectless materials, etc.

Constructing NEMS can be possible utilizing two main approaches: *self-assembly* and *manipulation*. Several laboratories especially in the fields of chemistry (supramolecular chemistry) and biology are trying to use this approach to build nano structures and devices [5]. This approach is promising in building higly-repetitive or symmetrical structures, but is unlikely to produce, by itsely, the asymmetric structures needed in nano machinery, and they are ill-suited for rapid prototyping. Latter approach utilizes knowledge from macrorobotic manipulation and assembly with the physics and chemistry of nanoscale phenomena [6], [2].

In this paper, manipulation approach is selected, and the term *nano manipulation* is defined as the manipulation of *nanometer* size objects with a nano robot that has a *micro/nanometer* size end-effector and *(sub/)nanometer* resolution manipulation/position control. By the manipulation, it is meant that nano objects are pushed or pulled, cut, picked and placed, assembled, drilled, etc. Manipulation in the nanometric scale world is in the very preliminary stage, and the aim of this paper is to survey previous work, define main issues, and to propose a macro to nano telemanipulation (M2NT-m) system. By constructing such a telemanipulation system, manipulation of objects with sizes ranging from 1 *nm* - 10 *μm* is to be realized, and the immature knowledge of micro/nano forces during nano manipulation is aimed to be improved and understood more clearly by analytical and experimental models. Future target is automatic nano manipulation systems which are indispensible for the industrial applications.

2 Prior Work

Groupings of nano manipulation systems can be conducted based on the utilized operation technics such as teleoperation or automatic manipulation, or utilized nano manipulator. In the former grouping, a human operator manipulates the nano objects by using a man-machine user interface. The operator controls the nano robot directly or sends task commands to the nano robot controller as shown in Figure 1. In the direct teleoperation system, the user interface can consist of visual, tactile or force feedback. Hollis et al. [3] used only tactile feedback from the nano world. In [2], force feedback and 3-D real-time Virtual Reality graphics display interface are utilized during manipulation. Direct approach can realize tasks requiring high-level intelligence and flexibility. However, it is slow, not precise, not exactly repeatable, and engaged in many complex and challenging scale difference problems. On the other hand, the task-oriented approach avoids these problems by executing only the given tasks in a closed-loop autonomous control. There is no report on task-oriented approach in the nano scale. In the other manipulation group, the automatic approach, nano robot has a closed-loop control using sensory information. It is utilized by Ramachandran et al. [6], Schaefer et al. [7]. However, the automatic control in the nano world seems to be very challenging and not reliable at present due to the complexity of the nano physics, changing environmental effects and insufficient intelligent strategies.

In the view of utilized nano manipulator, there are two

0-7803-4503-7/98/$10.00 1998 IEEE

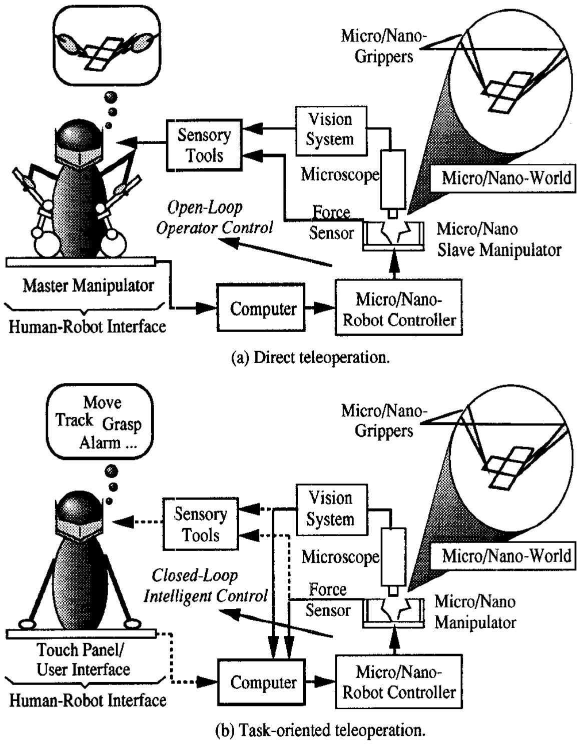

Figure 1: Direct teleoperation and task-oriented teleoperation.

main groups: STM-based and AFM-based manipulation systems. STM measures the tunneling current between its metallic probe and sample while scanning in x-y direction. On the other hand, AFM has a cantilever with a very sharp tip such that the cantilever deflection or vibration resonant frequency are changed due to the attractive or repulsive interatomic forces between the tip and sample atoms. Controlling these changes, the magnitude of normal and lateral forces can be obtained directly or indirectly. Comparing these microscopes, STM has a better lateral resolution, i.e. STM probe interacts with less number of sample atoms, while AFM has a large interaction range. This property makes STM attractive for very local manipulation tasks such as manipulation of atoms or molecules [9] by applying voltage pulses between the probe and sample. On the other hand, AFM can only realize more mechanical tasks such as push and pull [7], [4], [6]. However, AFM has more application areas since it is applicable to any conducting or non-conducting material while STM can be used only for conducting or semi-conducting materials. Furthermore, STM gives only 3-D topology data, but AFM can provide both topology and interaction force data. This point is very advantageous in AFM for reliable force feedback from the nano world to the macro world.

3 Main Issues

Main issues in the M2NT-m system which is shown in Figure 2 can be defined in terms of the macro system (human-machine interface, master manipulator, etc.), the macro to nano interface system (teleoperation, positioning devices and control, micro-tool fabrication, and micro vision), and the nano system (sensing devices, nano physics, and nano manipulator).

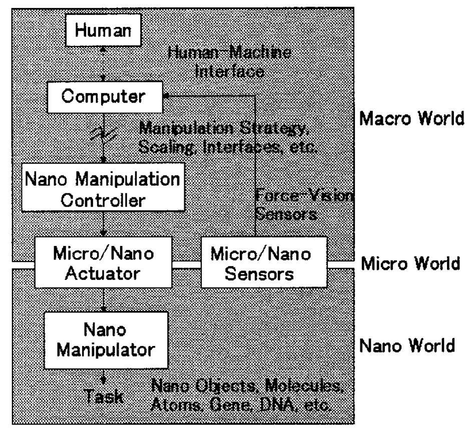

Figure 2: The structure of a teleoperated nano manipulation system.

In teleoperation systems, the human-interface enables the operator to sense the nano world and try to realize the given task in a user-friendly way. Such an interface should include a visualization tool and a manipulation tool. The aspects of the visualization tool are: (1) 3-D interactive visualization using virtual reality or other technologies: actively and locally/globally rotating, zooming, and viewpoint changing depending on the operator head or eye motion, (2) User-friendly: easy to visualize and not preventing operator's motion capabilities, (3) Multiresolution and tunable range: using micro and nano vision sensors together with variable physical zooming.

Besides of seeing the nano world, feeling the nano forces is the other most important issue for reliable task execution. For this purpose, a haptic device can be used to feel the forces in the operator's hand, and to function as the master manipulator to teleoperate the slave nano manipulator. Here, the properties of the haptic device are: (1) 3 positioning and force feedback joints, (2) light and fastly reactive for feeling instant force changes, (3) high force update rates (around 1 KHz) for realistic feeling of surfaces/textures, (4) long and tunable force range (around 0-5 N), (5) haptic device independent software design, (6) easy to interface with the rest of the system.

In the teleoperation part, the motions of the operator is to be scaled to the nano world slave manipulator motions using a stable and robust controller. The reverse direction is also needed for force feedback to the operator. Therefore, a bilateral teleoperation controller is to be designed. Besides of this low-level control, a scaling control is needed to scale the nano forces to the macro scale and vice verca. There are geometric, impedance, time and power scaling approaches in the literature for the macro to micro teleoperation systems [10]. Finally, a high-level control approach is required for realistic feeling of the nano forces. At this point, intermediate representations can be designed.

As the micro/nano actuator in the precision positioning of the nano manipulator, piezoelectric actuators are the most preferred ones. The main requirements are: (1) coarse and fine positioning with long range, (2) at least 3 DOF (x-y-z), (3) smallest resolution must be around 0.1 nm at the z-direction and 1 nm at the x and y directions.

In the micro world, optical microscope (OM) is helpful in the sense of providing a low-resolution image of the nano manipulator and the object in a large field of view. The maximum empirical resolution of the conventional OMs is around 0.5 μm. The trade-off here is between the resolution and the field of view (FOV). High resolution means small FOV. Also, another problem is the working distance of the OM; (distance between its lens and the nano tool). High resolution means small working distance which puts mechanical constraints to the system.

In the nano world, the first main part is the nano manipulator. Depending on the application and task, different manipulators are to be designed. But, for the beginning, manipulators for pick and place, pulling and pushing, drilling, cutting like tasks are required. As the nano manipulator AFM cantilever or STM metal tip can be utilized.

The most challenging problem in the nano world is the nano physics where the gravity laws in macro world changes to the attractive and repulsive interatomic forces. These forces can be investigated in two groups: contact and non-contact forces. Contact means that the manipulator and the particle distance is less than around 0.3 nm. In this range, repulsive and attractive interatomic forces such as van der Waals, triboelectrification, surface tension and chemical bonding exist. We are in the domain of quantum mechanics and chemistry in the atomic scale. The noncontact forces are mainly attractive forces such as van der Waals, electrostatic, and hydrodynamic forces. Analytical models of both contact and noncontact forces are highly nonlinear and complex, and depend on the empirical parameters which can change easily by environmental conditions. Therefore, the best way is comparing those analytical models with the experimental results and refining them. Furthermore, environmental effects such as temperature change, dust, humidity, and vibration must be controlled as much as possible for avoiding unexpected results.

4 System Overview

The proposed M2NT-m system is shown in Figure 3. In the macro scale, a 1-DOF haptic device with position and force sensors is mounted on a standard mouse such that it has 3-DOF position and 1-DOF force feedback. Operator puts his/her hand to the tip of the 1-DOF parallel arm, applies the normal force $F_{op}(t)$ while feeling the arm motion, $x_m(t)$. Meanwhile, he/she can move the mouse for moving the sample in the x-y plane. Furthermore, besides of the force display, a 3-D Virtual Reality interface enables a real-time visual display for the operator. The details of the visual display are given in [8].

In the nano world, AFM cantilever is utilized as a nano scale manipulator and the position and force sensor. In this study, only push and pull manipulation tasks for 2-D positioning/assembly of spherical particles are taken into consideration. Thus, the main mechanism of the nano manipulator is given in Figure 4. A particle which is called *absorbate* '*a*' from now on is placed on a *substrate* '*s*' initially. Then, the cantilever *tip* '*t*' is contacted by the particle by a teleoperation control. After contact, the interatomic and surface repulsive forces $F_{ta}(t)$ and $F_{as}(t)$ and frictional forces $f_{ta}(t)$ and $f_{as}(t)$ act on the absorbate. Due to the cantilever deflection detection type, only the normal force on the cantilever tip can be measured. Therefore, only this force is felt on the operator hand in our system.

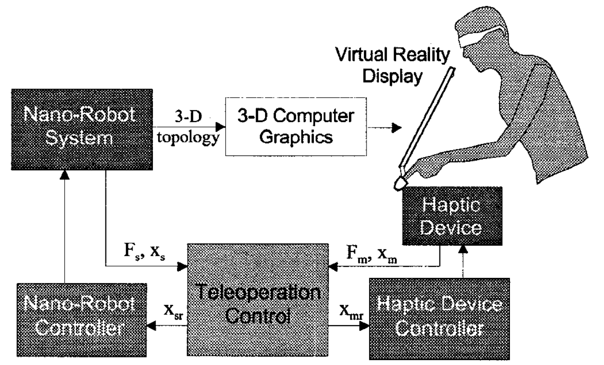

Figure 3: The overall M2NT-m system.

The force model of the contact system can also be viewed as a mass-spring system as shown in Figure 5. The spring constants k_{ca} and k_{as} and damping constants b_{ca} and b_{as} represent the interaction forces. For positioning the particle, our strategy is as follows: "use the fixed cantilever as stopper while moving the substrate under the particle with a uniform speed." Here, the constraint for realizing a reliable positioning is given as follows:

- *in manipulation mode:* while the tip approaches to and retracts from the particle, or it fixes the particle, the particle should always stay in its original position.
- *in imaging mode:* while getting the 3-D image of the particles using the AFM, the cantilever tip should not touch to the particles since it can change their positions. Thus, the images should be acquired in noncontact mode type of AFM imaging [7] for *nm* size particles, or another sensor such as Opticle Microscope can be used in the case of μm size particles.

For the first constraint, following conditions should be held:

$$F_{ta}(t)cos\theta + f_{ta}(t)sin\theta = f_{as}(t), \quad (1)$$
$$F_{ta}(t)sin\theta + F_{as}(t) \geq f_{ta}(t)cos\theta. \quad (2)$$

Here, the frictional forces can be controlled for satisfying above conditions by selecting proper materials, controlling environmental conditions such as humidity, and controlling the point of contact $g(t)$ anf tip force on the absorbate $F_{ta}(t)$ by changing $x_s(t)$ via the teleoperation control. The first two are fixed before the manipulation experiment. Therefore, during the experiment only $x_s(t)$ can be changed by the operator for successfull operation.

4.1 Nano Forces

The nano forces $F_{ta}(t)$ and $F_{as}(t)$ consist of the van der Waals, capillary, electrostatic forces, and repulsive forces due

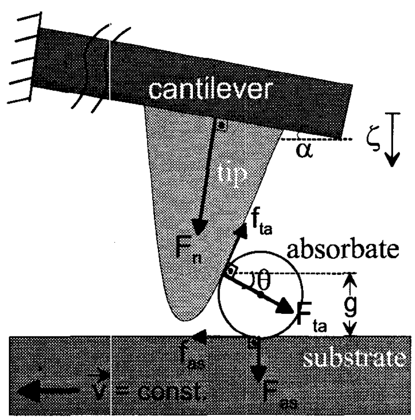

Figure 4: 2-D contact manipulation of spherical particles by the cantilever tip and forces acting on the particle.

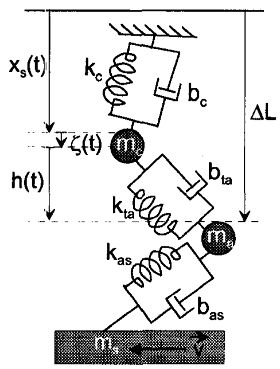

Figure 5: Mass-spring model of the contact manipulation.

to the contact such as indentation force, chemical forces, etc. For simplicity, no electrostatic forces is assumed (which can be partially realized by grounding the substrate if it is conducting). Since the absorbate and sample can be assumed not to change their initial contact position, F_{as} can be modeled as

$$F_{as} = 4\pi\gamma R_a + \frac{AR_a}{6a_0^2}, \quad (3)$$

where R_a is the particle radius, A is the Hamacker constant, a_0 is the interatomic distance, and γ is the surface energy constant of the liquid layer. Here, '+' force means attractive and '-' force do repulsive force.

The tip-absorbate force $F_{ta}(t)$ changes at each instant depending on the separation distance $h(t)$ such that

$$\begin{aligned}
F_{ta}(t) &\approx 0, if \quad h(t) > 100nm, \\
F_{ta}(t) &= \frac{A\widetilde{R}}{6h(t)^2}, if \quad 100nm \geq h(t) > H, \\
F_{ta}(t) &= \frac{A\widetilde{R}}{6h(t)^2} + \frac{2\pi\gamma\widetilde{R}cos\delta}{1+\frac{h(t)}{d}}, if \quad H \geq h(t) > a_0, \\
F_{ta}(t) &= \frac{A\widetilde{R}}{6a_0^2} + 2\pi\gamma\widetilde{R} - \frac{8}{3}\frac{E\sqrt{\widetilde{R}}}{1-\nu^2}(a_0 - h(t))^{3/2}, \\
&\approx c_1 + c_2 h(t), if \quad a_0 \geq h(t) > h_{max}, \quad (4)
\end{aligned}$$

where $\widetilde{R} = R_a R_t/(R_a + R_t)$, R_t is the tip radius, h_{max} is the maximum distance where after the plastic deformation begins (normally this limit should not be exceeded during manipulation for not desired deformations on the particle and the tip), E is the Young's modulus and ν is the Poisson's coefficient of the substrate, c_1 and c_2 are experimentally computed constants of the contact linear region, H is the thickness of the liquid layer, and δ and d are shown in Figure 6.

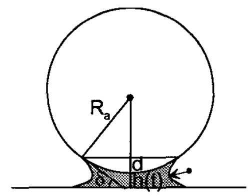

Figure 6: Capillary force due to the liquid layer on surfaces.

The frictional forces are generally modeled as the combination of Amonton's-like load based friction and the area of contact dependent adhesion controlled friction [1] such that

$$f(t) = cA(t) + \mu L(t), \quad (5)$$

where μ and c are constants for a given system, $A(t)$ is the true contact area, and $L(t)$ is the normal load. For controlling, i.e. minimizing, the friction, μ, c, $A(t)$ and $L(t)$ parameters should be controlled, i.e. minimized. Here, c is predominantly a surface energy contribution which can be controlled by adjusting parameters that effect the adhesion forces between the surfaces. μ is primarily geometry dependent such that it can be minimized by having smooth surfaces without asperities. Thus, if there is any deformation on the surfaces μ also changes. On the other hand, the normal loads $L_{ta}(t)$ and $L_{as}(t)$ are given as follows:

$$\begin{aligned}
L_{ta}(t) &= f_{as}(t)cos\theta - F_{as}(t)sin\theta - F_{ta}(t), \quad (6) \\
L_{as}(t) &= F_{ta}(t)sin\theta + F_{as}(t) - f_{ta}(t)cos\theta. \quad (7)
\end{aligned}$$

For the contact area, the following formulation is assumed (JKR deformation model [1]) for a sphere-to-sphere contact case:

$$\begin{aligned}
A_{ta}(t) &= \pi\left(\frac{\widetilde{R}L(t)}{K}\right)^{2/3}, \quad if \quad \gamma = 0, \\
A_{ta}(t) &= \pi\Big\{\frac{\widetilde{R}}{K}[L(t) + 3\pi\widetilde{R}\gamma + (6\pi\widetilde{R}\gamma L(t) + \\
&\quad (6\pi\widetilde{R}\gamma)^2)^{1/2}]\Big\}^{2/3}, \quad if \quad \gamma > 0, \quad (8)
\end{aligned}$$

where K is the elastic modulus of the materials. $A_{as}(t)$ can be computed by replacing $\gamma \to 2\gamma$ and $\widetilde{R} \to R_a$. Thus, $f_{ta}(t)$ and $f_{as}(t)$ can be written as:

$$\begin{aligned}
f_{ta}(t) &= c_{ta}A_{ta}(t) + \mu_{ta}L_{ta}(t), \\
f_{as}(t) &= c_{as}A_{as}(t) + \mu_{as}L_{as}(t). \quad (9)
\end{aligned}$$

Finally, the normal force acting on the cantilever is computed as:

$$F_n(t) = f_{ta}(t)cos(\theta - \alpha) - F_{ta}(t)sin(\theta - \alpha). \quad (10)$$

4.2 Master and Slave Dynamics

In the master haptic device, the dynamics of the arm due to the operator force $F_{op}(t)$ and haptic device can be given as:

$$M_m\ddot{x}_m(t) + B_m\dot{x}_m(t) = F_{op}(t) - \tau_m(t), \quad (11)$$

where $\tau_m(t)$ is the torque generated by the haptic device motor. In our design, a linear DC motor is used such that its model is given as

$$C(s) = \frac{X(s)}{E_a(s)} = \frac{K_m}{s(T_m s + 1)}K_p. \quad (12)$$

Here, $X(t)$ is the displacement of the motor shaft, E_a is the applied armature voltage, $T_m = 0.0011sec$, $K_m = 29.41(rad/sec)/V$, and $K_p = 2.79 \times 10^{-5}$. In the low-level control of the motor a proportional controller with constant $G = 10000$ is utilized where the closed loop transfer function becomes as

$$X_m(s)/X_{mr}(s) = M(s) = \frac{C(s)G}{1 + C(s)G} = \frac{a^2}{s^2 + bs + a^2} \quad (13)$$

where $b = 1/T_m$, $a^2 = GK_mK_p/T_m$, and $x_{mr}(t)$ is the reference master position.

For the cantilever, $F_n(t)$ results in the following dynamics:

$$F_n(h(t)) = m_c\ddot{\zeta}(t) + b_c\dot{\zeta}(t) + k_c\zeta(t), \quad (14)$$

where $\zeta(t)$ is the tip deflection from the equilibrium position, $h(t) = \Delta L - x_s(t) - \zeta(t)$ is the tip-absorbate distance, m_c, b_c and k_c are the cantilever mass, damping constant and spring constant respectively. Assuming a slow motion of the cantilever, the cantilever is assumed to reach to its equilibrium state at each time instant. In this case, the dynamics becomes as

$$F_n(h(t)) = k_c\zeta(t). \quad (15)$$

On the other hand, $F_n(t)$ is given in the equation (10) where it can be computed by using the equations (4) and (9). Here the relation between $F_s(t)$ and $x_s(t)$ can be held by putting $h(t) = \Delta L - x_s(t) - \zeta(t)$ in $F_s(h(t))$. Here, this relation is highly nonlinear in the *noncontact* region, i.e. $h(t) > a_0$, and becomes linear only in the *contact* region until there is a plastic deformation.

4.3 Bilateral Teleoperation Control

From the manipulation model, it can be seen that the operator should control the cantilever contact z-position while feeling the normal interaction force between the tip and particle on his/her hand using the haptic device. Also the operator will decide the direction of the horizontal x-y motion of the substrate using the mouse. Since the latter does not include any force feedback, the aim of the teleoperation system is taken as to feel the normal nano force $F_n(t)$ on the operator hand while the operator determines the z-position $x_s(t)$ of the cantilever as shown in Figure 7. The teleoperation problem can be defined as to design a controller such that as $t \to \infty$:

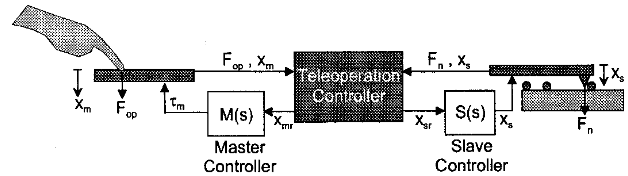

Figure 7: Bilateral force feedback teleoperation control system.

- *Condition 1.* $x_m \to \alpha_p x_s$,
- *Condition 2.* $F_m \to \alpha_f F_s$,

where $F_m(t) = F_{op}(t)$ and $F_s(t) = F_n(t)$ are the master and slave forces, $x_m(t)$ and $x_s(t)$ are the master and slave positions, and α_p and α_f are scaling constants for the position and force respectively.

A bilateral teleoperation controller generates the necessary position or force reference values for the master and slave low-level controllers at each step for enabling the above conditions of the teleoperation control. There are different approaches such as force-position, position-force or impedance shaping teleoperation control. From these approaches, the first two are utilized in this study. For the force-position case, the desired torque applied to the operator $\tau_{mr}(t)$, and the desired slave position $x_{sr}(t)$ are generated using following equations:

$$\tau_{mr}(t) = -\alpha_f F_s(t) - K_f(\alpha_f F_s(t) - F_m(t)), \quad (16)$$
$$x_{sr}(t) = K_p(\alpha_p x_m(t) - x_s(t)) - K_v\dot{x}_s(t), \quad (17)$$

where K_p and K_v are PD control constants, and K_f is the force gain constant. On the other hand, for the position-force control approach, the reference master position and slave forces are given as:

$$x_{mr}(t) = K_p(x_m(t)/\alpha_p - x_m(t)) - K_v\dot{x}_m - F_m(t) \quad (18)$$
$$F_{sr}(t) = \frac{F_m(t)}{\alpha_f} + K_f(\frac{F_m(t)}{\alpha_f} - F_s(t)). \quad (19)$$

In the preliminary experiments, cantilever force $F_s(t)$ vs. $x_s(t)$ relation is held where the tip is approaching and retracting from a mica substrate. From the Figure 8, the linear behaviour after the contact point C can be observed clearly. Here, the c_1 and c_2 constants are computed as 0.86 and -34.06 for the approaching and 0.67 and -25.17 for the retraction of the tip. Also, the adhesion force of the surface can be observed such that the maximum adhesion force occurs at the pull-off point A where $F_s \approx 4\pi\gamma R_t$. A low-speed approaching and retracting of the cantilever tip to a mica sample by the control of constant operator force is simulated by the force-position teleoperation control approach. In this simulation slave controller is open-loop and $\alpha_p x_{mr} = x_s$ is assumed. From the Figure 9, the master and slave forces converge to the same value which means that

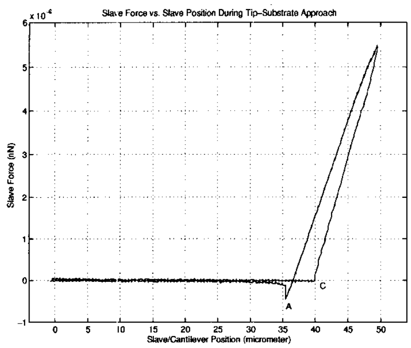

Figure 8: Experimantal force vs. cantilever distance curve during approaching to and retracting from a mica sample.

the controller enables a reliable feedback. The simulation parameters are $\alpha_p = 15 \times 10^{-9}$, $\alpha_f = 4 \times 10^6$, $M_m = 0.1kg$, $B_m = 100Nsec/m$, $K_f = 100$, $A = 1e - 19$, $R_t = 25nm$, $a_0 = 3.49A^o$, $E = 0.05GPa$, $\nu = 0.3$, and $k_c = 30N/m$. In the figure, the F_s vs. x_s curve is shown where it is similar to the experimental force-distance curve by the exception of very little hysteresis behaviour. Finally, the master controller tracking is shown such that $x_m(t)$ tracks the reference $x_{mr}(t)$.

5 Conclusion

In this paper, issues of the macro to nano telemanipulation systems are introduced, and a telemanipulation system that uses AFM as the nano manipulator and sensor is proposed. is introduced. Modeling and control of the spherical particle manipulation, and dynamical models of the AFM cantilever and haptic device dynamics have been realized. Besides of 3-D visual feedback in the user interface, a 1DOF haptic device has been constructed for nano scale tactile sensing and generating motion commands for the AFM. Introducing teleoperation control system approach, 2-D particle assembly applications can be held. 2-D assembly of nano particles on a flat surface by push and pull operations for understanding the chemical, electrical and mechanical properties of specific materials, and construction of nano devices. Preliminary experiments and simulations on AFM and teleoperation system show that the system can be utilized for tele-nanomanipulation experiments.

References

[1] A. Berman and J. Israelachvili. Control and minimization of friction via surface modification. *Micro/Nano Tribology and its Application, Kluwer Academics Pub.*, pages 317–329, 1997.

[2] M. Falvo, R. Superfine, S. Washburn, and et al. The nanomanipulator: A teleoperator for manipulating materials at the nanometer scale. In *Proc. of the Int. Symp. on the Science and Technology of Atomically Engineered Materials*, pages 579–586, Nov 1995.

[3] R. L. Hollis, S. Salcudean, and D. W. Abraham. Toward a telenanorobotic manipulation system with atomic scale force feedback and motion resolution. In *IEEE Int. Conf. on MicroElectromechanical Systems*, pages 115–119, 1990.

[4] T. Junno, K. Deppert, L. Montelius, and L. Samuelson. Controlled manipulation of nanoparticles with an atomic force microscopy. *App. Physics Letters*, 66(26):3627–3629, June 1995.

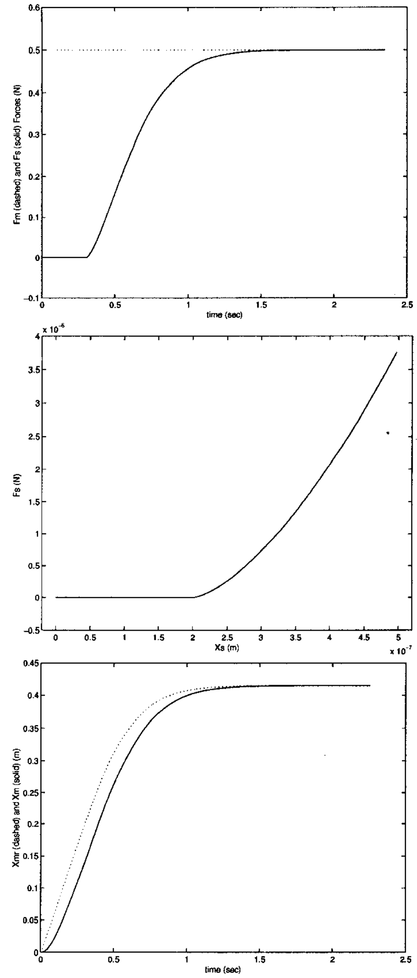

Figure 9: Simulated slave and master force, slave force and position and master reference and actual position results during approaching to a mica sample by the control of a constant operator force.

[5] J.M. Lehn. Supramolecular chemistry and nanotechnology. In *France-Japan Workshop on from Nano to Macroscale Science and Technology through Micro Systems*, pages 14–15, Apr. 1997.

[6] T. R. Ramachandran, A. Madhukar, P. Chen, and B. E. Koel. Imaging and direct manipulation of nanoscale three-dimensional features using the non-contact atomic force microscope. *J. Vac. Sci. Technol. B*, 1997.

[7] D.M. Schafer, R. Reifenberger, A. Patil, and R.P. Andres. Fabrication of two-dimensional arrays of nanometric-size clusters with the atomic force microscopy. *App. Physics Letters*, 66(8):1012–1014, Feb. 1995.

[8] M. Sitti, Satoshi Horiguchi, and H. Hashimoto. Nano telemanipulation using virtual reality interface. In *IEEE Int. Symp. on Industrial Electronics*, (to be published) 1998.

[9] J.A. Stroscio and D.M. Eigler. Atomic and molecular manipulation with the scanning tunneling microscope. *Science*, 254(5036):1319–1326, Nov. 1991.

[10] Hiroki Tokashiki, Prasad Akella, and Kazuo Tanie. Scaled bilateral telemanipulation: An experimental investigation of scaling laws. In *SPIE*, pages 214–224, 1994.